Supporting Information

Synthesis and characterization of azobenzene molecular glasses with different glass transition temperatures

Austin Diggins[a], Eoin Dawson[a], Mahnaz Kamaliardakani[b], Christian Pellerin[b], Ribal Georges Sabat[a] and Olivier Lebel[c]

[a] Department of Physics and Space Science, Royal Military College of Canada, PO Box 17000, Station Forces Kingston, Ontario CANADA, K7K 7B4

[b] Département de chimie, Université de Montréal, C.P. 6128, succursale Centre-ville, Montréal, Québec, CANADA, H3C 3J7

[c] Department of Chemistry and Chemical Engineering, Royal Military College of Canada, PO Box 17000, Station Forces Kingston, Ontario CANADA, K7K 7B4

*Corresponding author: c.pellerin@umontreal.ca, sabat@rmc.ca, Olivier.Lebel@rmc.ca

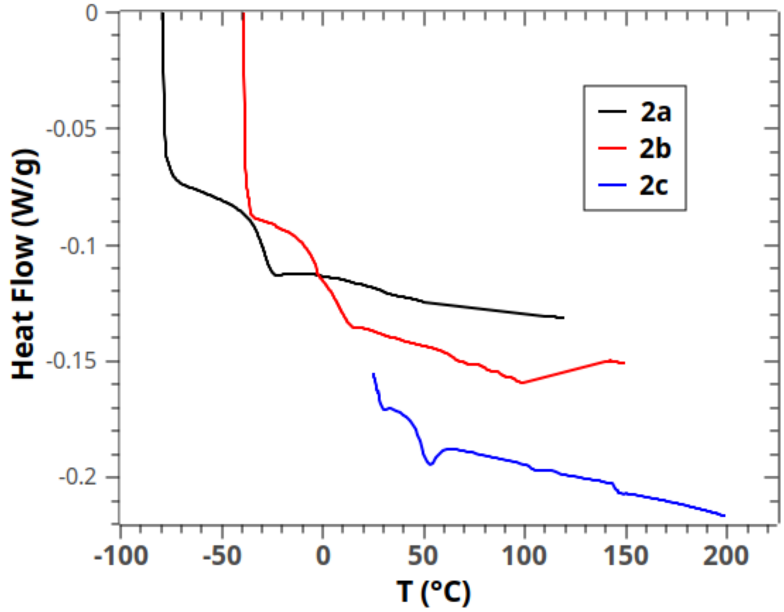

Figure S1. DSC thermograms of precursors **2a-c**. The thermograms were recorded at a heating rate of 5 °C/min after a preliminary heating run to erase the thermal history. Exotherms are facing up.

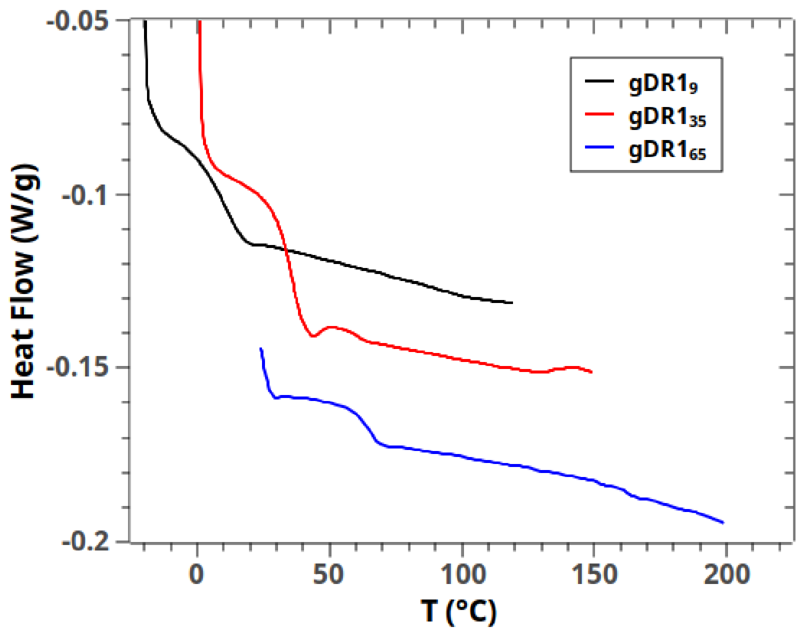

Figure S2. DSC thermograms of **gDR1$_9$**, **gDR1$_{35}$** and **gDR1$_{65}$**. The thermograms were recorded at a heating rate of 5 °C/min after a preliminary heating run to erase the thermal history. Exotherms are facing up.

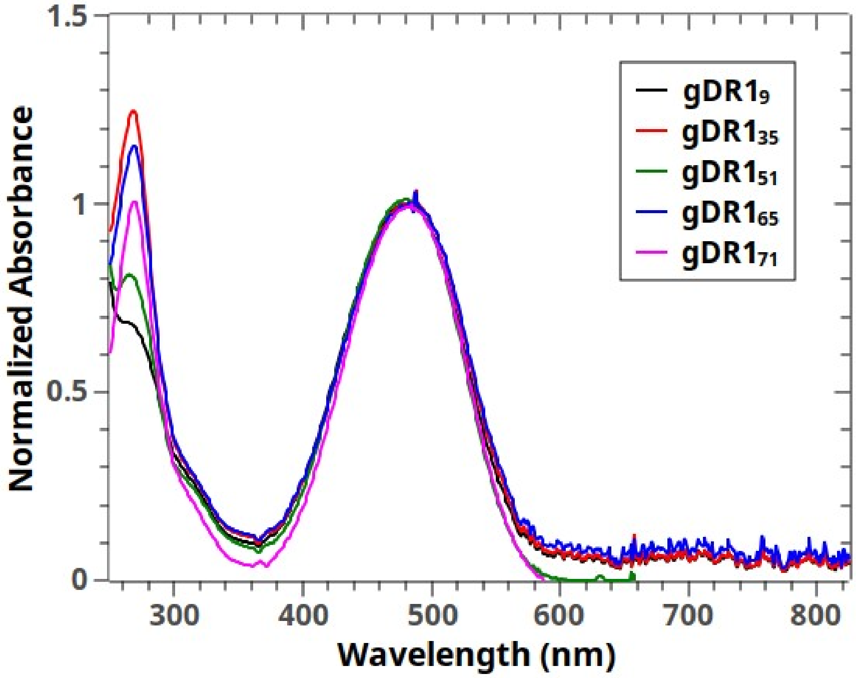

Figure S3. Normalized UV-Visible spectra of the different **gDR1$_{Tg}$** analogues used in the present study. Spectra were recorded in 0.01 mM solution in CH_2Cl_2.

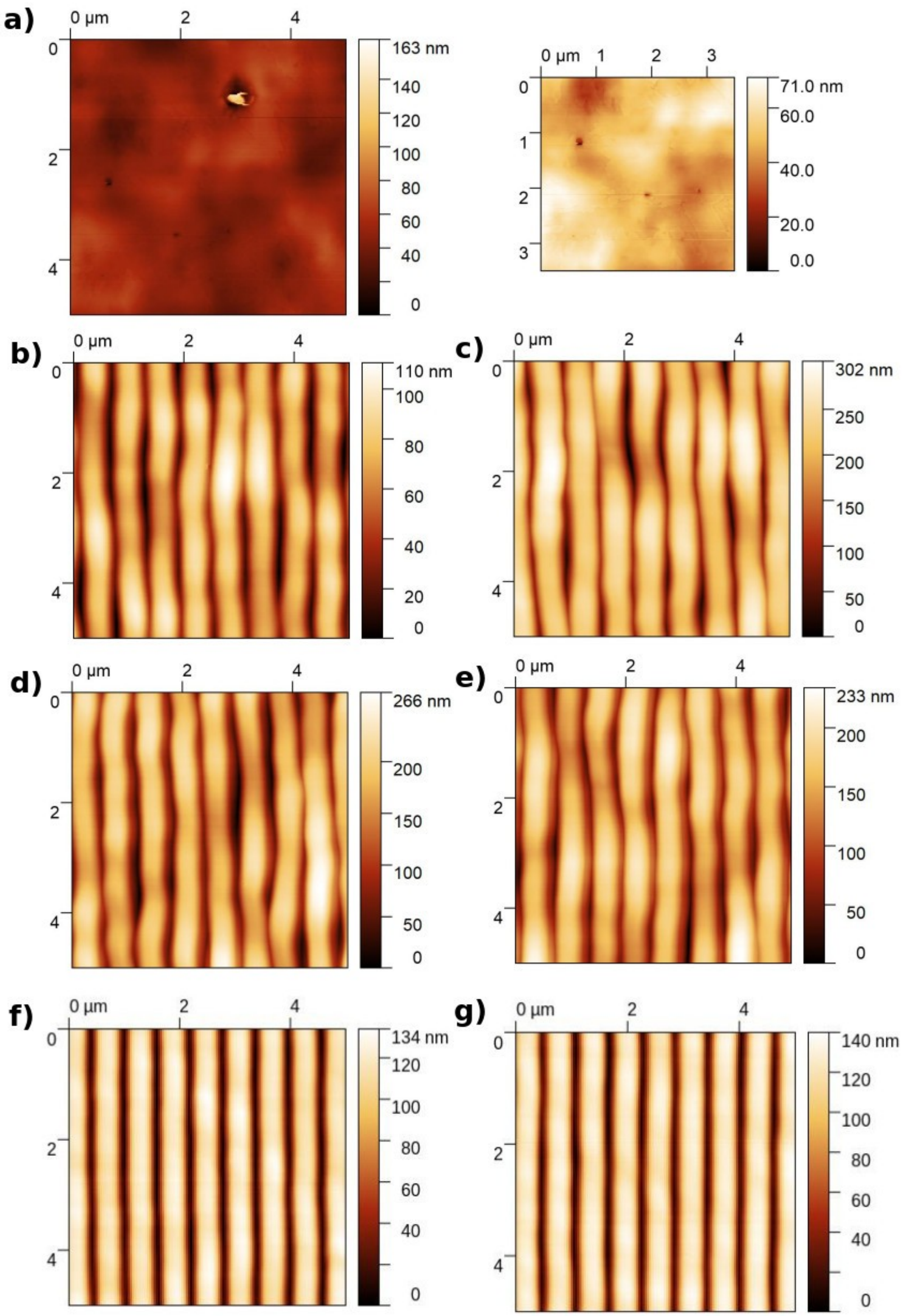

Figure S4. Atomic Force Microscopy (AFM) scans of thin films of **gDR1$_{Tg}$** after irradiation with a 488 nm laser at an irradiance of 100 mW/cm^2. (a) **gDR1$_9$** after 200 s irradiation; (b) **gDR1$_{35}$** after 200 s irradiation; (c) **gDR1$_{51}$** after 600 s irradiation; (d) **gDR1$_{65}$** after 600 s irradiation; (e) **gDR1$_{71}$** after 800 s irradiation; (f) **gDR1$_{65}$** after 60 irradiation (at 300 mW/cm^2); (g) **gDR1$_{71}$** after 150 s irradiation. The AFM scan for **gDR1$_9$** was recorded 2 h after irradiation was stopped. A cropped image where the surface defect is not shown is also included for (a). The images in (b)-(e) likely show a distortion of the gratings due to the longer irradiation times, as the gratings shown in images (f)-(g), which had not yet reached saturation, do not show such defects.

Table S1. Initial SRG inscription rates for **gDR1$_{Tg}$** with a 488-nm laser, obtained from the linear regression of the DE plots in Figure 1, before they plateaued.

Compound	**Irradiance (mW/cm^2)**	**Inscription rate (DE %/s)**	
gDR1$_9$	100	0.01226	$\pm 8 \times 10^{-5}$
	200	0.0248	$\pm 2 \times 10^{-4}$
	300	0.0338	$\pm 8 \times 10^{-4}$
gDR1$_{35}$	100	0.01514	$\pm 5 \times 10^{-5}$
	200	0.0405	$\pm 2 \times 10^{-4}$
	300	0.044	$\pm 1 \times 10^{-3}$
gDR1$_{51}$	100	0.0680	$\pm 1 \times 10^{-4}$
	200	0.1417	$\pm 6 \times 10^{-4}$
	300	0.0752	$\pm 7 \times 10^{-4}$
gDR1$_{65}$	100	0.0666	$\pm 1 \times 10^{-4}$
	200	0.1395	$\pm 5 \times 10^{-4}$
	300	0.151	$\pm 1 \times 10^{-3}$
gDR1$_{71}$	100	0.0575	$\pm 1 \times 10^{-4}$
	200	0.1149	$\pm 3 \times 10^{-4}$
	300	0.202	$\pm 1 \times 10^{-3}$

Table S2. Initial SRG inscription rates for **gDR1$_{Tg}$** with a 532-nm laser, obtained from the linear regression of the DE plots in Figure 1, before they plateaued.

Compound	**Irradiance (mW/cm^2)**	**Inscription rate (DE %/s)**	
gDR1$_9$	100	0.00272	$\pm 2 \times 10^{-5}$
	200	0.00175	$\pm 5 \times 10^{-5}$
	300	0.0112	$\pm 1 \times 10^{-4}$
gDR1$_{35}$	100	0.01279	$\pm 3 \times 10^{-5}$
	200	0.0298	$\pm 2 \times 10^{-4}$
	300	0.02655	$\pm 9 \times 10^{-5}$
gDR1$_{51}$	100	0.0532	$\pm 1 \times 10^{-4}$
	200	0.0748	$\pm 3 \times 10^{-4}$
	300	0.0708	$\pm 2 \times 10^{-4}$
gDR1$_{65}$	100	0.05366	$\pm 6 \times 10^{-5}$
	200	0.0926	$\pm 3 \times 10^{-4}$
	300	0.092	$\pm 3 \times 10^{-3}$
gDR1$_{71}$	100	0.05014	$\pm 7 \times 10^{-5}$
	200	0.0846	$\pm 2 \times 10^{-4}$
	300	0.0762	$\pm 2 \times 10^{-4}$

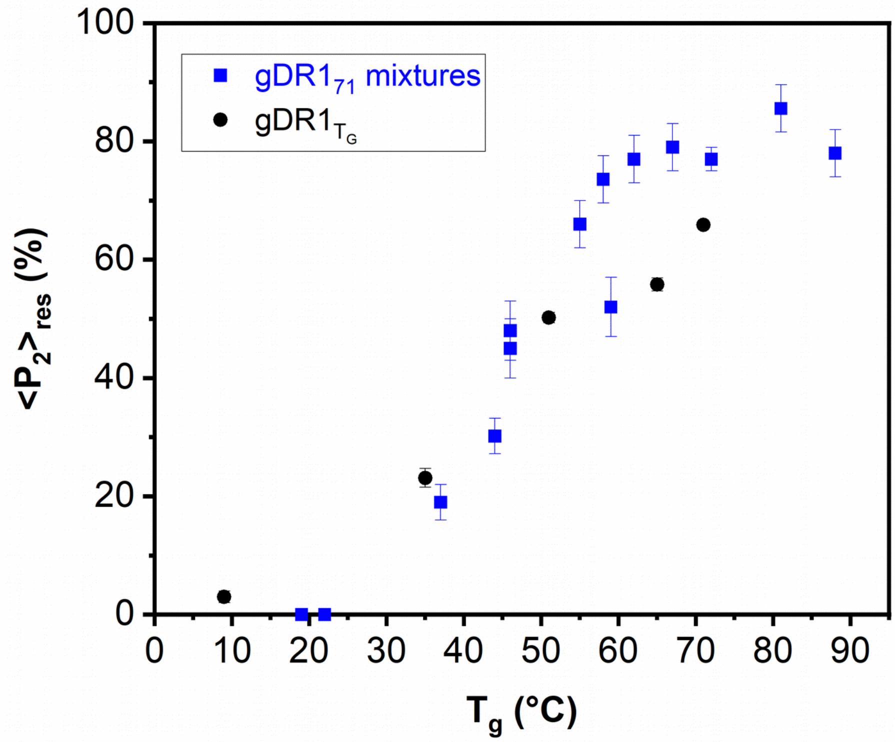

Figure S5. Effect of the glass transition temperature (T_g) on the residual orientation parameter ($\langle P_2 \rangle_{res}$) for pure gDR1$_{Tg}$ azo glasses (black) and for mixtures of azo glass gDR1$_{71}$ with photopassive glasses (blue). Similar trends are found for both cases. The mixtures results are reproduced from Ref. 24.

NMR Spectra of Compounds 1a-c, 2a-c, gDR1$_9$, gDR1$_{35}$ and gDR1$_{65}$

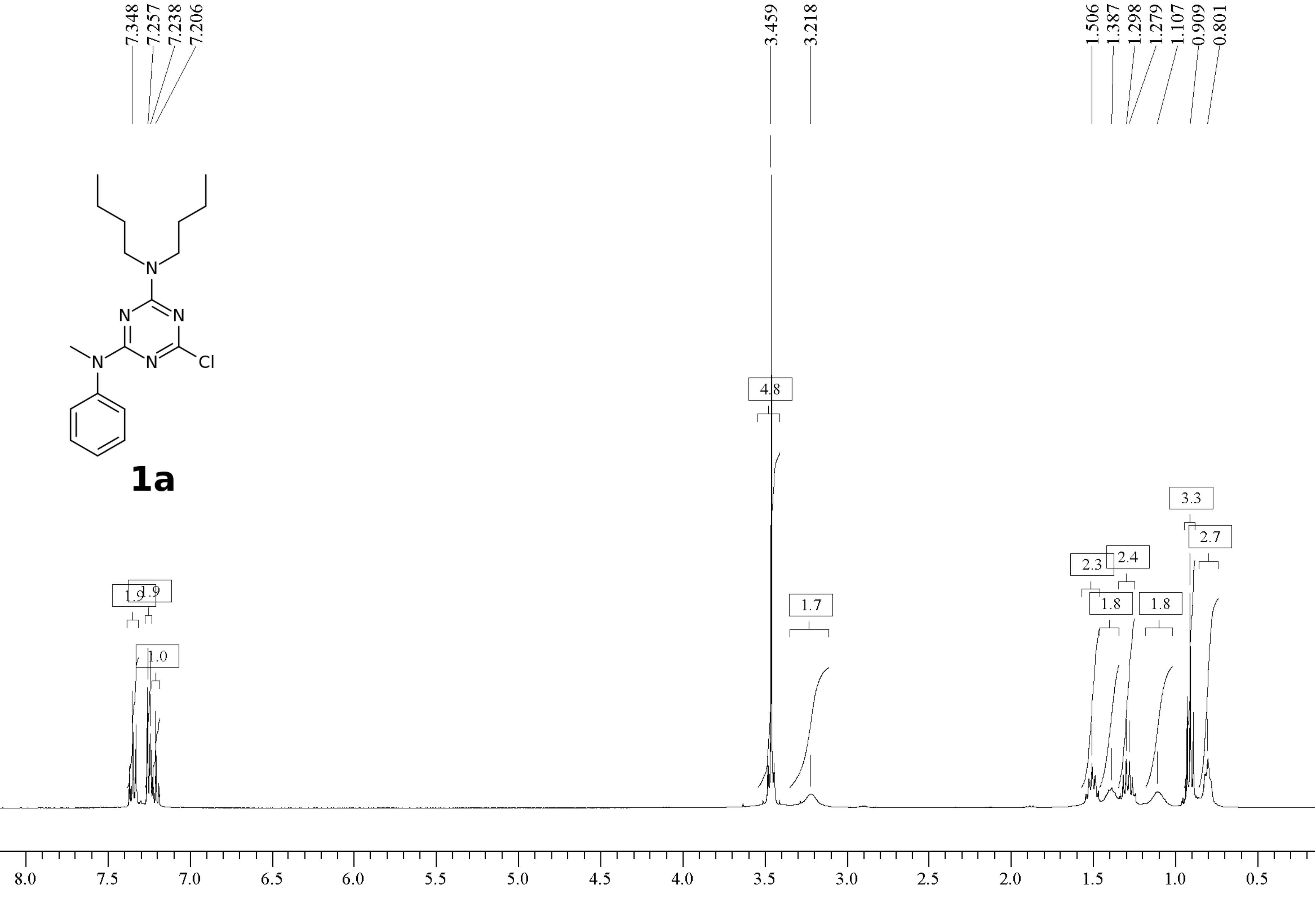
7.348
7.257
7.238
7.206
3.459
3.218
1.506
1.387
1.298
1.279
1.107
0.909
0.801
4.8
1.7
3.3
2.7
2.3
2.4
1.8
1.8
1.9
1.9
1.0
N
N
N
N
N
Cl
8.0
7.5
7.0
6.5
6.0
5.5
5.0
4.5
4.0
3.5
3.0
2.5
2.0
1.5
1.0
0.5

1a

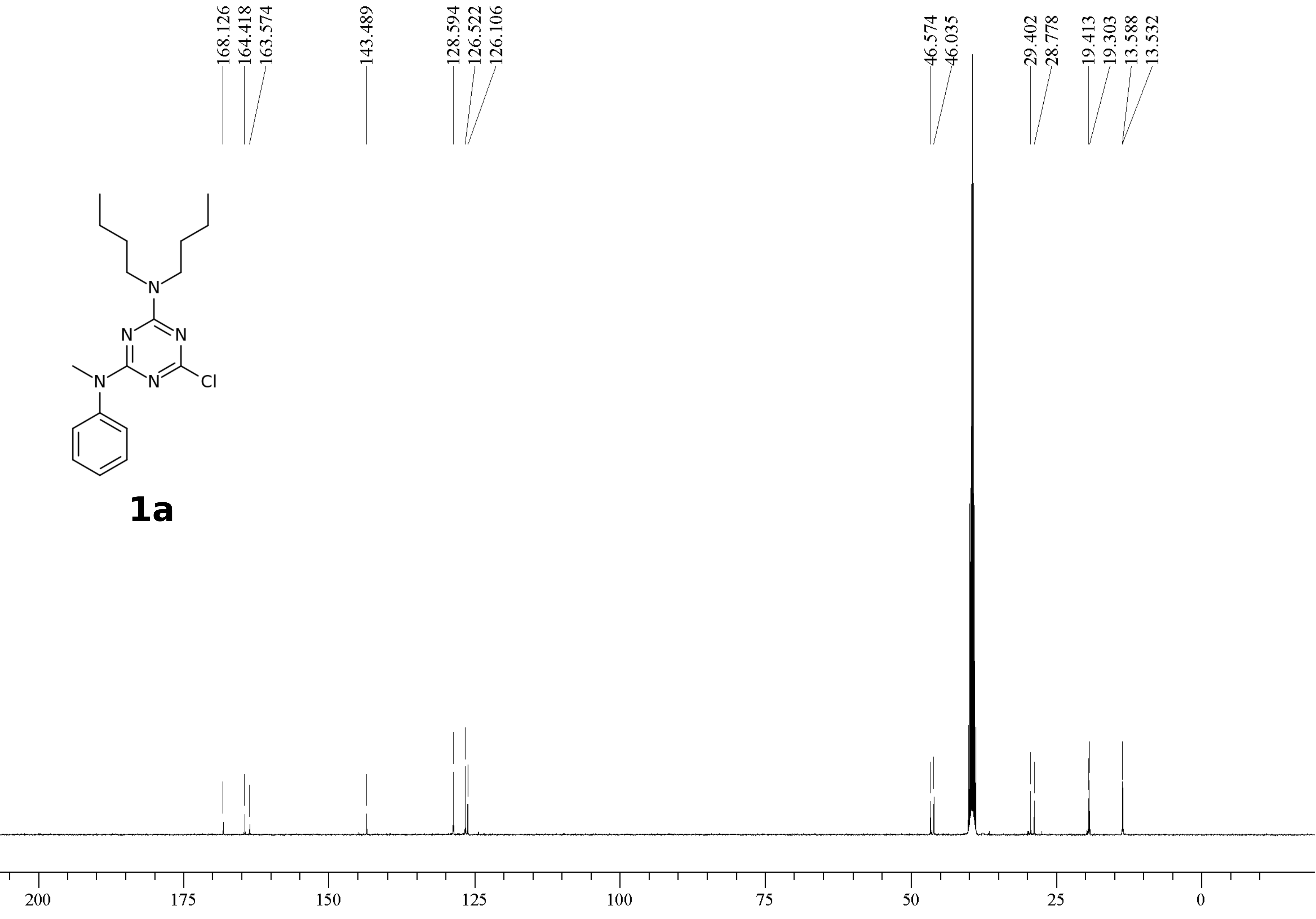
168.126
164.418
163.574
143.489
128.594
126.522
126.106
46.574
46.035
29.402
28.778
19.413
19.303
13.588
13.532
N
N
N
N
N
Cl
200
175
150
125
100
75
50
25
0

1a

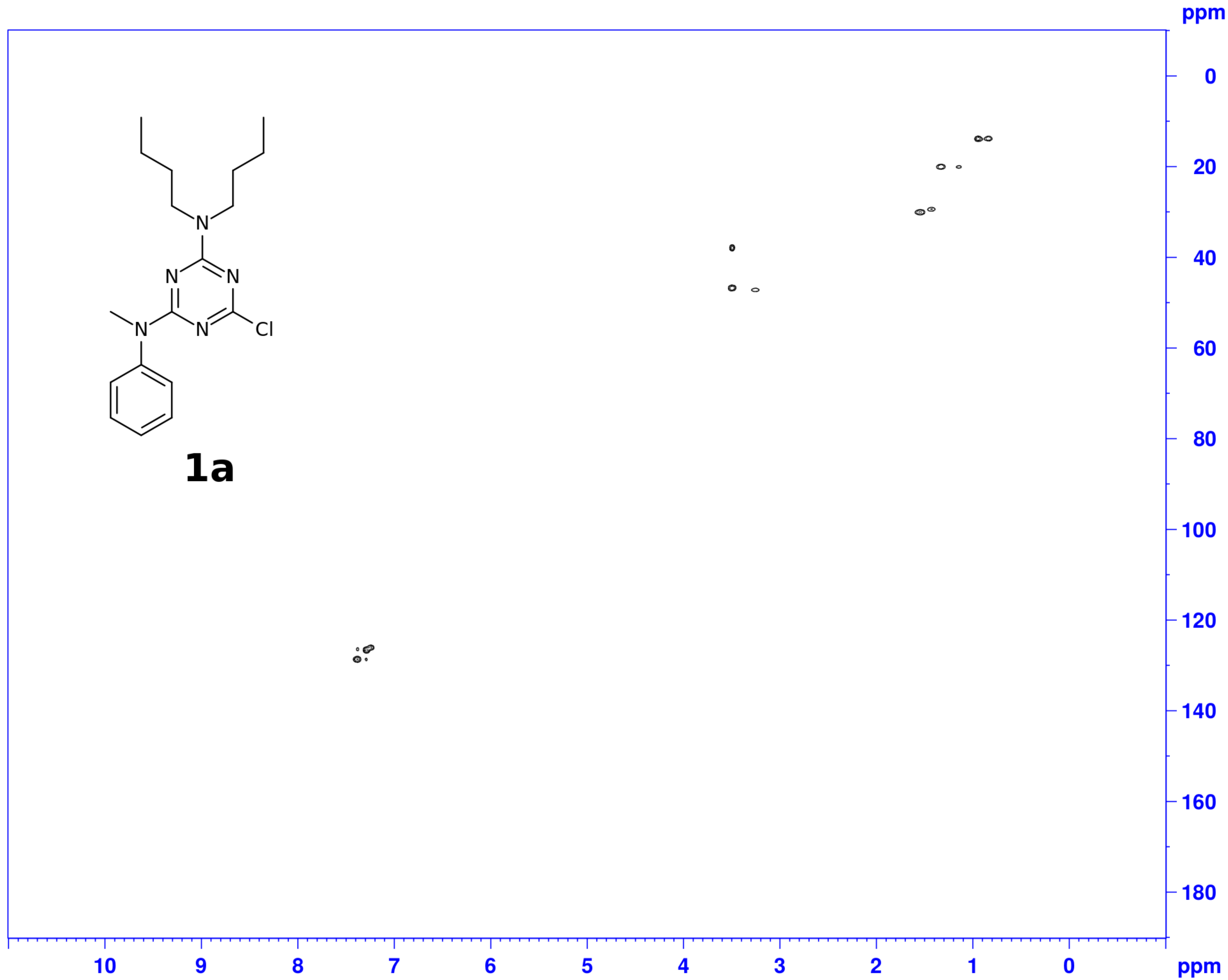

N
N
N
N
N
Cl
1a
ppm
0
20
40
60
80
100
120
140
160
180
ppm
10
9
8
7
6
5
4
3
2
1
0
ppm

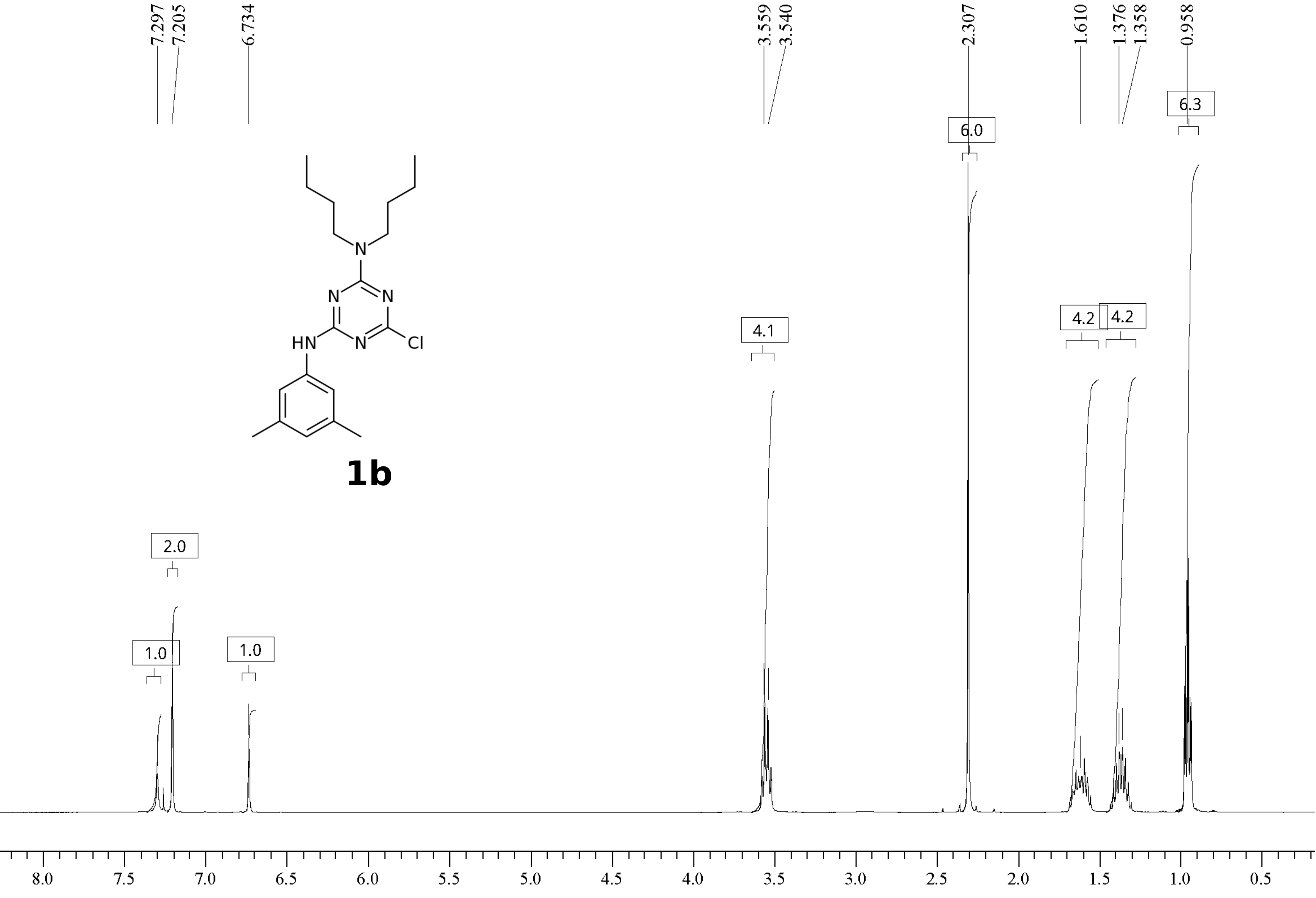
7.297
7.205
6.734
3.559
3.540
2.307
1.610
1.376
1.358
0.958
6.3
6.0
4.2
4.2
4.1
2.0
1.0
1.0
N
N
N
N
HN
Cl
1b
8.0
7.5
7.0
6.5
6.0
5.5
5.0
4.5
4.0
3.5
3.0
2.5
2.0
1.5
1.0
0.5

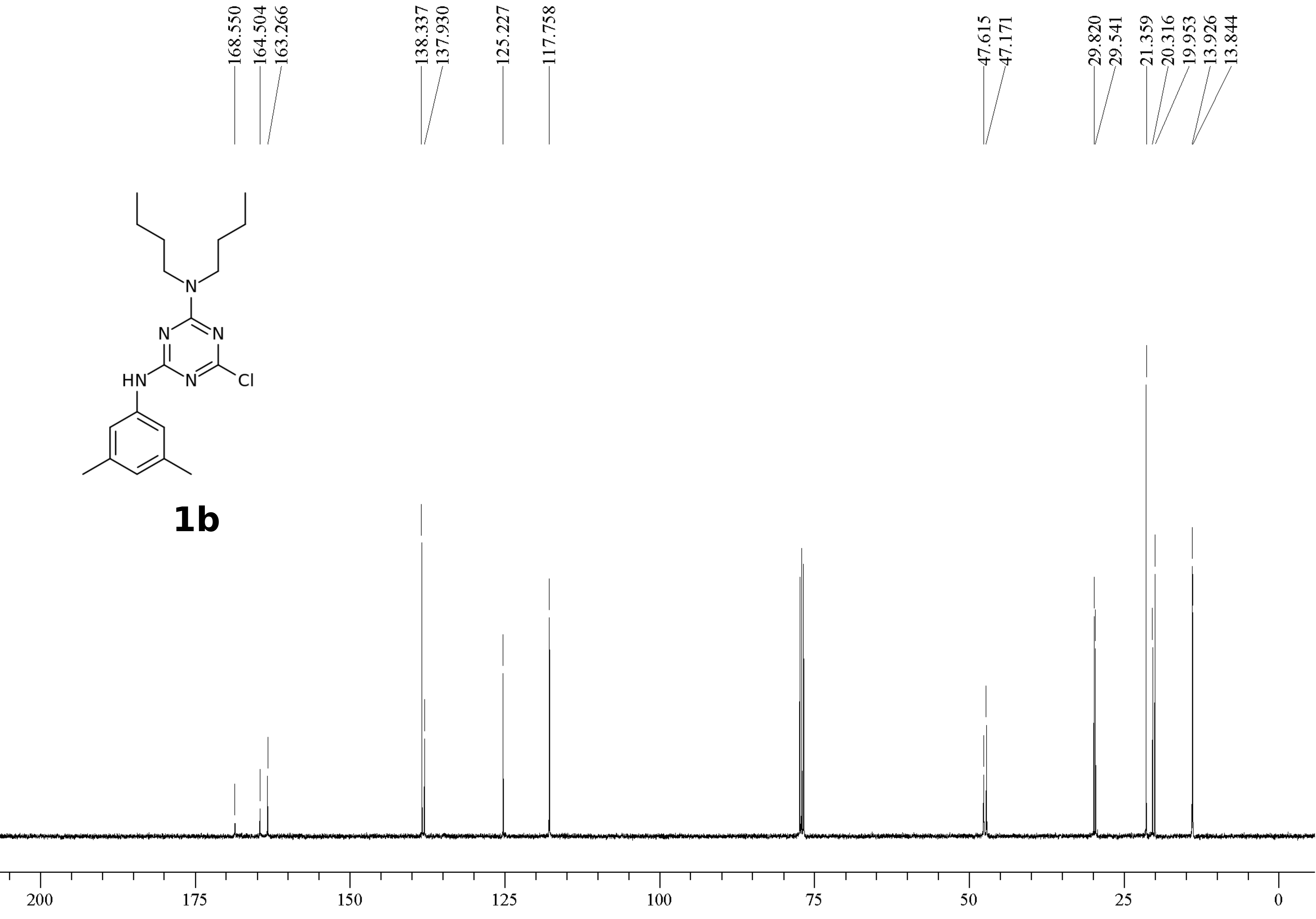

168.550
164.504
163.266
138.337
137.930
125.227
117.758
47.615
47.171
29.820
29.541
21.359
20.316
19.953
13.926
13.844
HN
N
Cl
200
175
150
125
100
75
50
25
0

1b

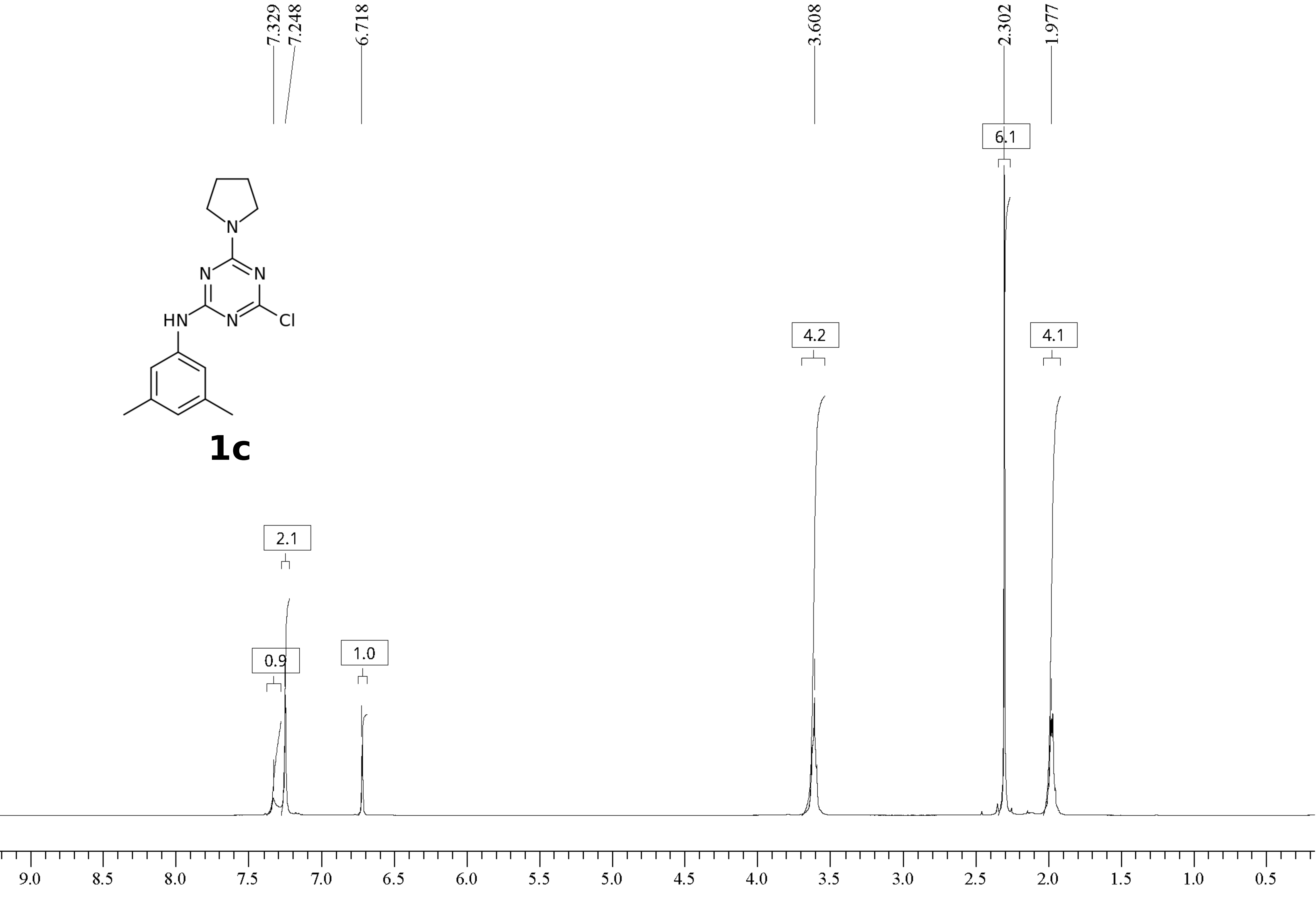
7.329
7.248
6.718
3.608
2.302
1.977
6.1
4.2
4.1
2.1
0.9
1.0
9.0
8.5
8.0
7.5
7.0
6.5
6.0
5.5
5.0
4.5
4.0
3.5
3.0
2.5
2.0
1.5
1.0
0.5

1c

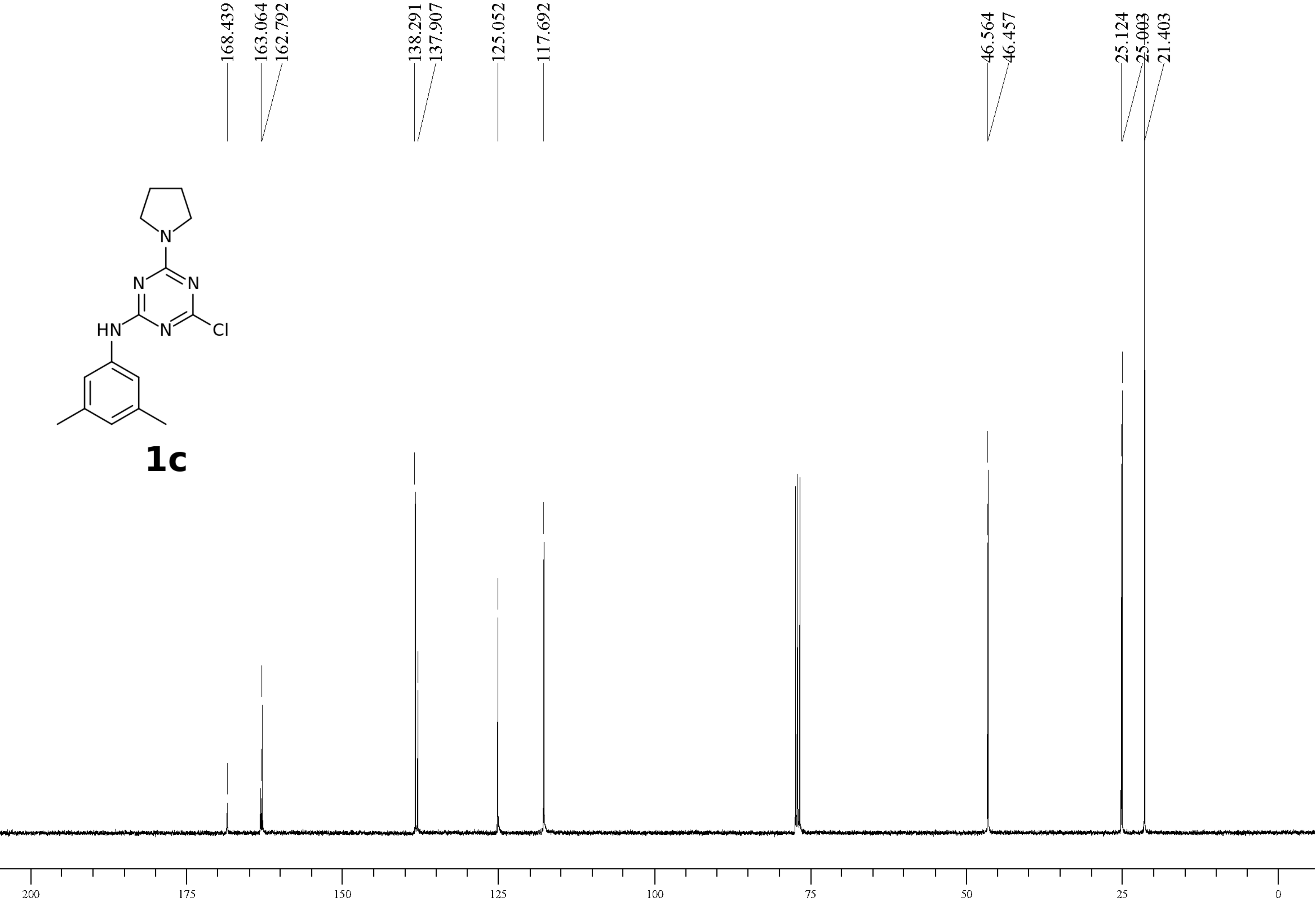

168.439
163.064
162.792
138.291
137.907
125.052
117.692
46.564
46.457
25.124
25.003
21.403
HN
N
Cl
1c
200
175
150
125
100
75
50
25
0

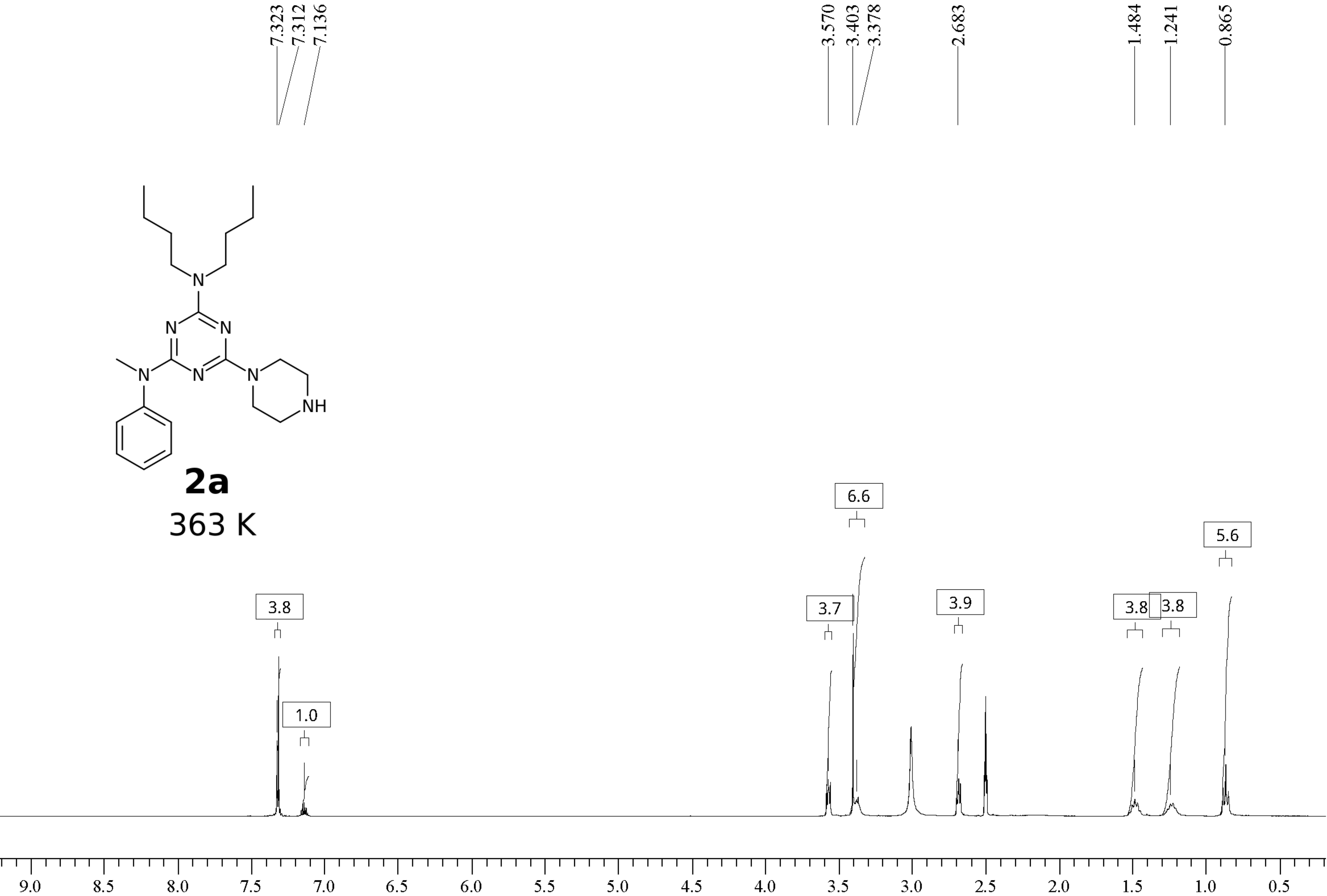
7.323
7.312
7.136
3.570
3.403
3.378
2.683
1.484
1.241
0.865
NH
N
3.8
1.0
3.7
6.6
3.9
3.8
3.8
5.6
9.0
8.5
8.0
7.5
7.0
6.5
6.0
5.5
5.0
4.5
4.0
3.5
3.0
2.5
2.0
1.5
1.0
0.5

2a
363 K

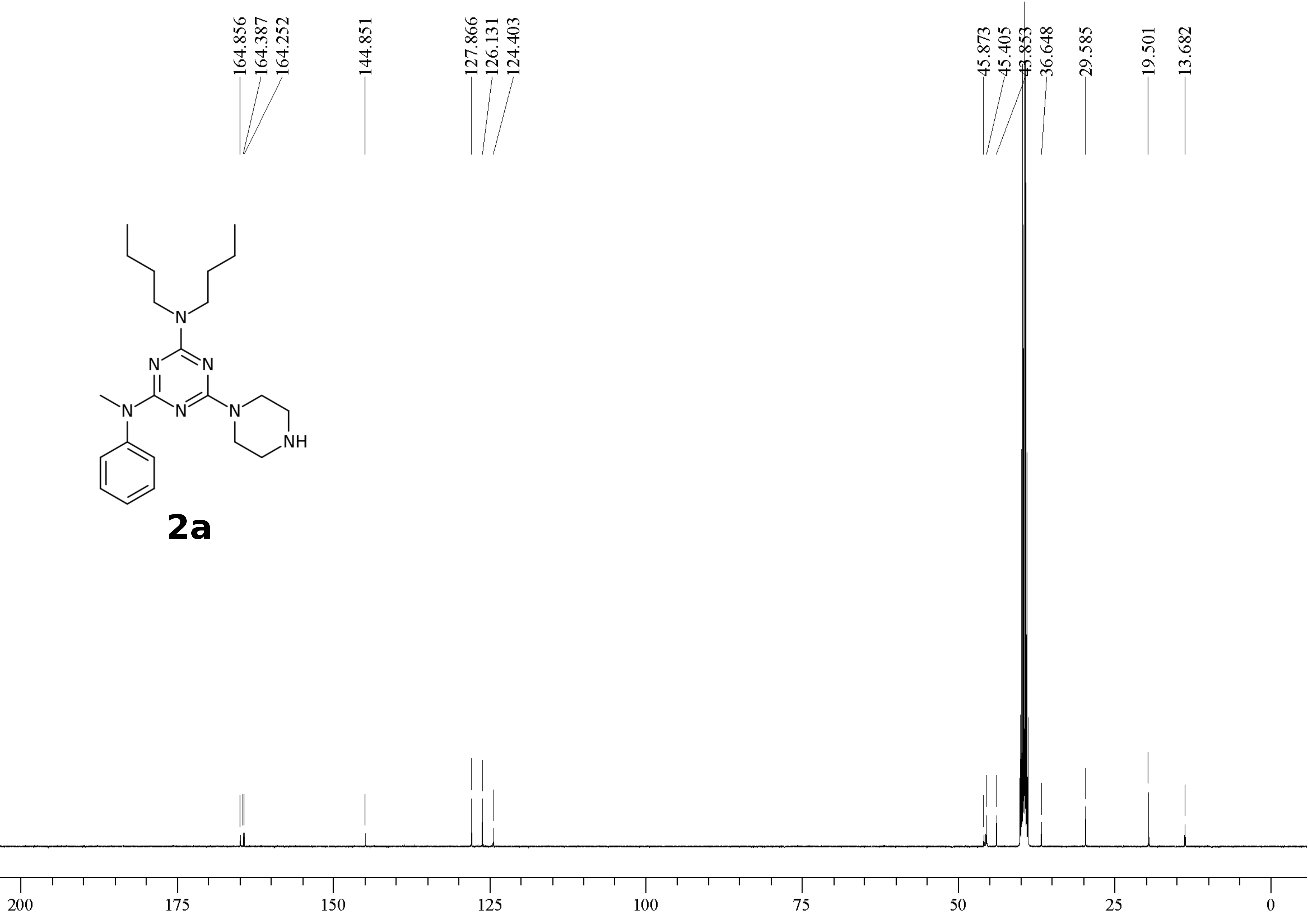
164.856
164.387
164.252
144.851
127.866
126.131
124.403
45.873
45.405
43.853
36.648
29.585
19.501
13.682
200
175
150
125
100
75
50
25
0
N
N
N
N
N
N
NH

2a

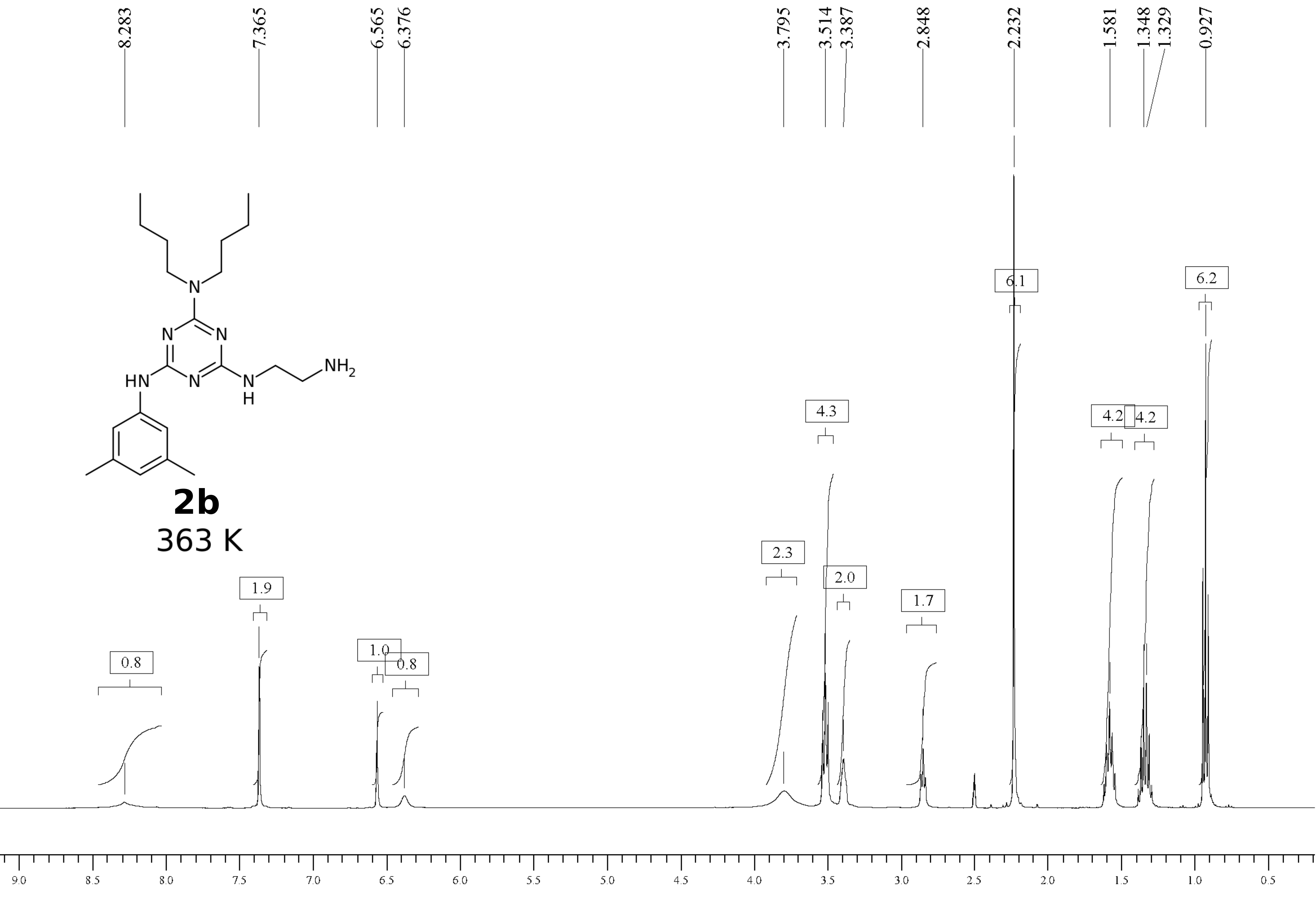
8.283
7.365
6.565
6.376
3.795
3.514
3.387
2.848
2.232
1.581
1.348
1.329
0.927
0.8
1.9
1.0
0.8
2.3
4.3
2.0
1.7
6.1
4.2
4.2
6.2
HN
N
N
N
N
NH2
H
2b
363 K
9.0
8.5
8.0
7.5
7.0
6.5
6.0
5.5
5.0
4.5
4.0
3.5
3.0
2.5
2.0
1.5
1.0
0.5

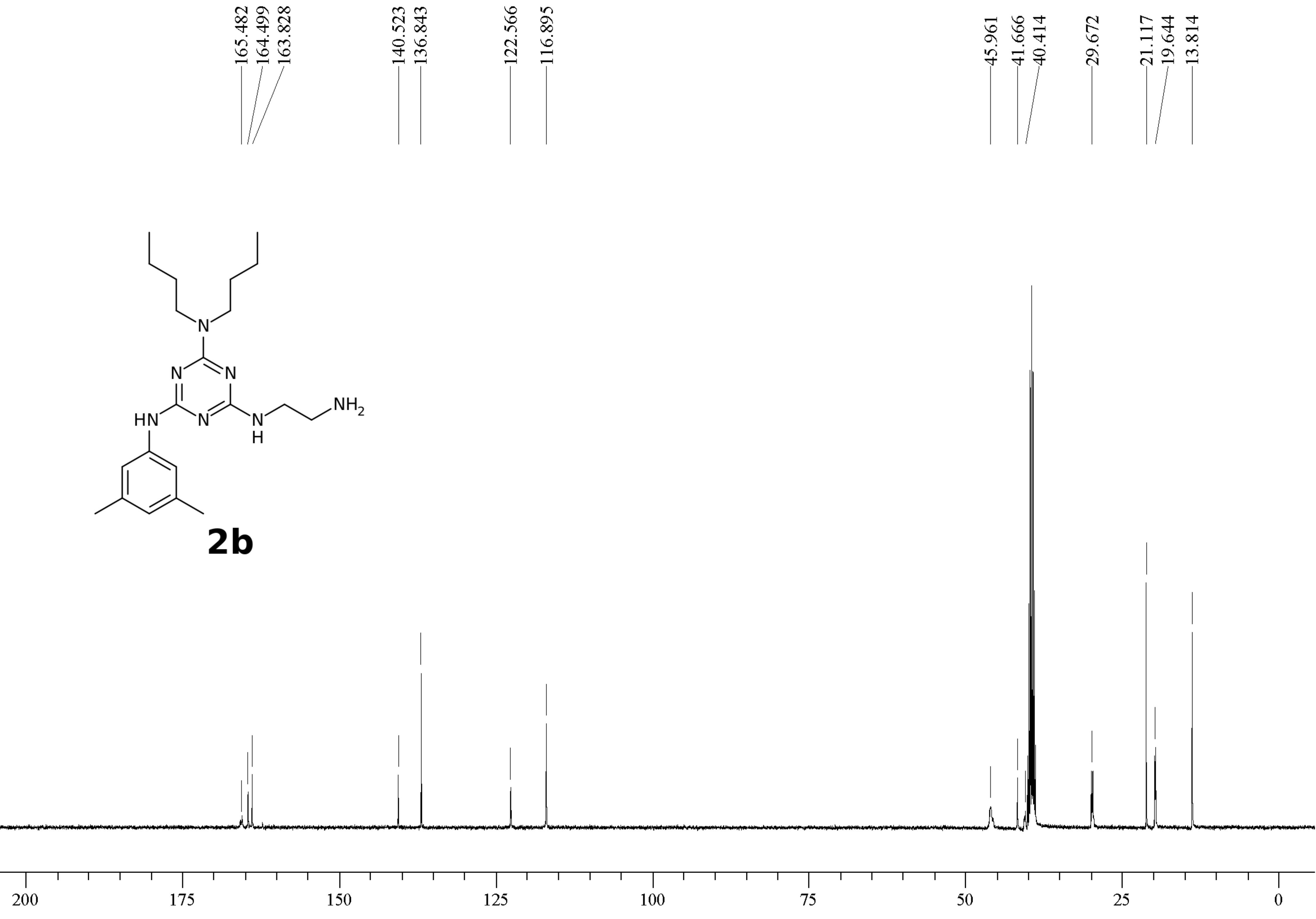
165.482
164.499
163.828
140.523
136.843
122.566
116.895
45.961
41.666
40.414
29.672
21.117
19.644
13.814
HN
N
N
N
N
H
NH2
2b
200
175
150
125
100
75
50
25
0

2c
363 K

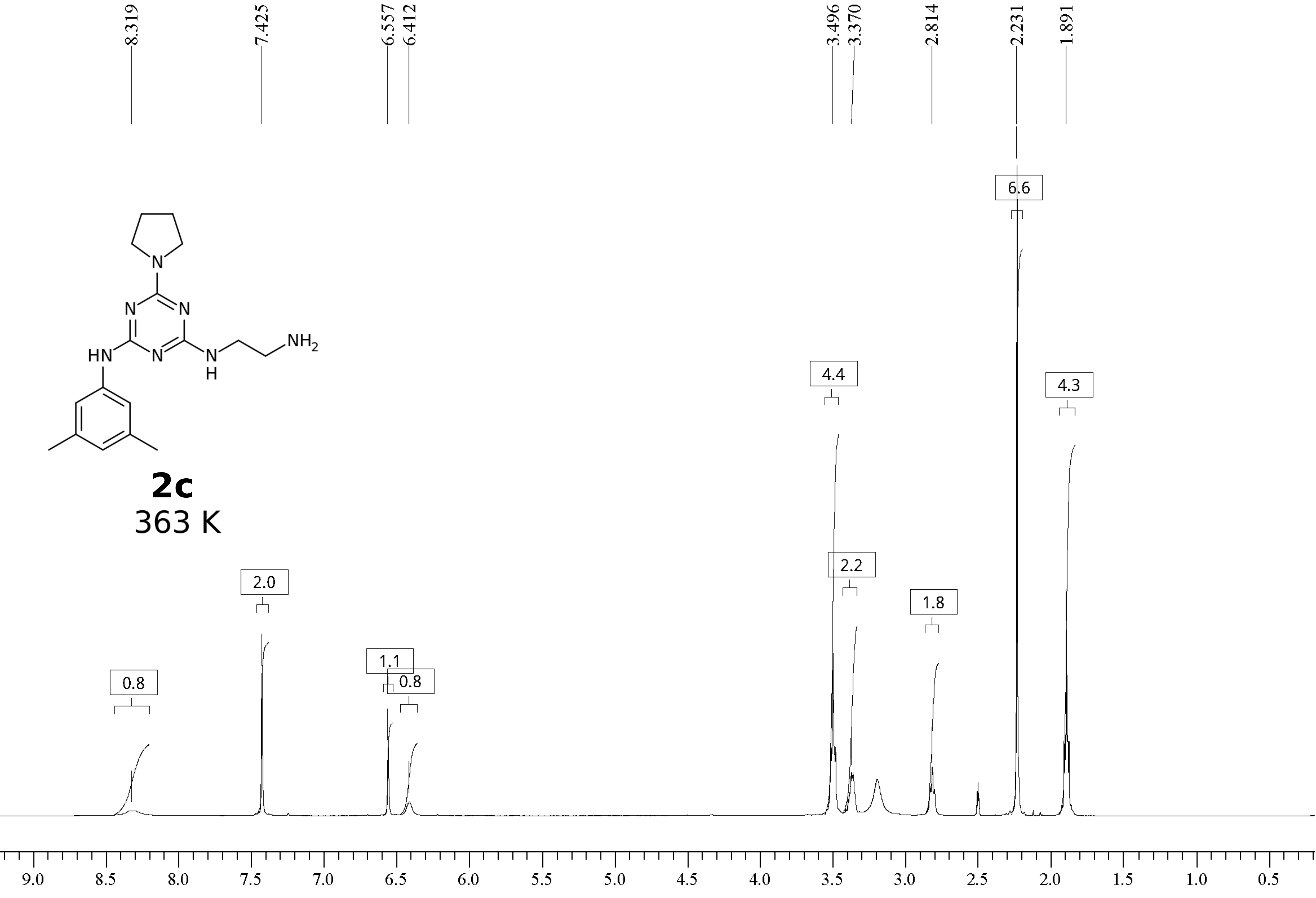
8.319
7.425
6.557
6.412
3.496
3.370
2.814
2.231
1.891
0.8
2.0
1.1
0.8
4.4
2.2
1.8
6.6
4.3
9.0
8.5
8.0
7.5
7.0
6.5
6.0
5.5
5.0
4.5
4.0
3.5
3.0
2.5
2.0
1.5
1.0
0.5

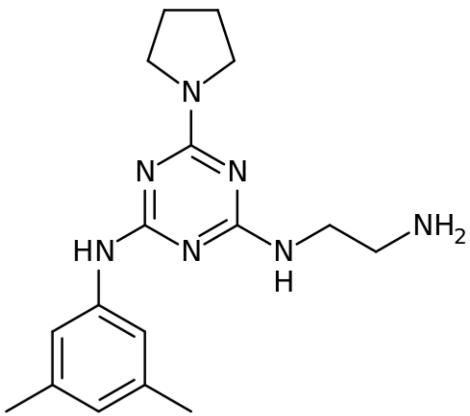

N
N
N
N
HN
N
H
NH2

2c

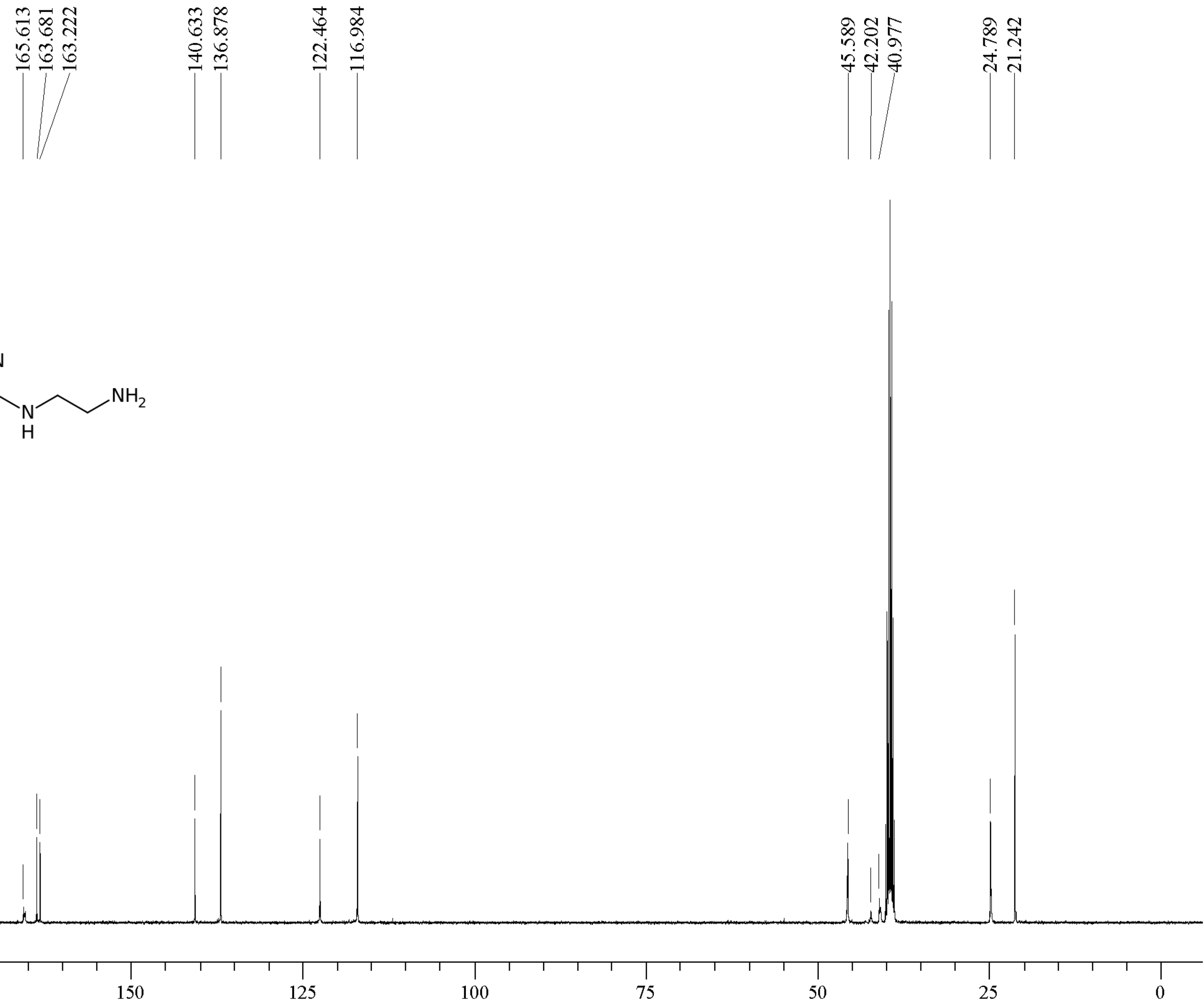

165.613
163.681
163.222
140.633
136.878
122.464
116.984
45.589
42.202
40.977
24.789
21.242
200
175
150
125
100
75
50
25
0

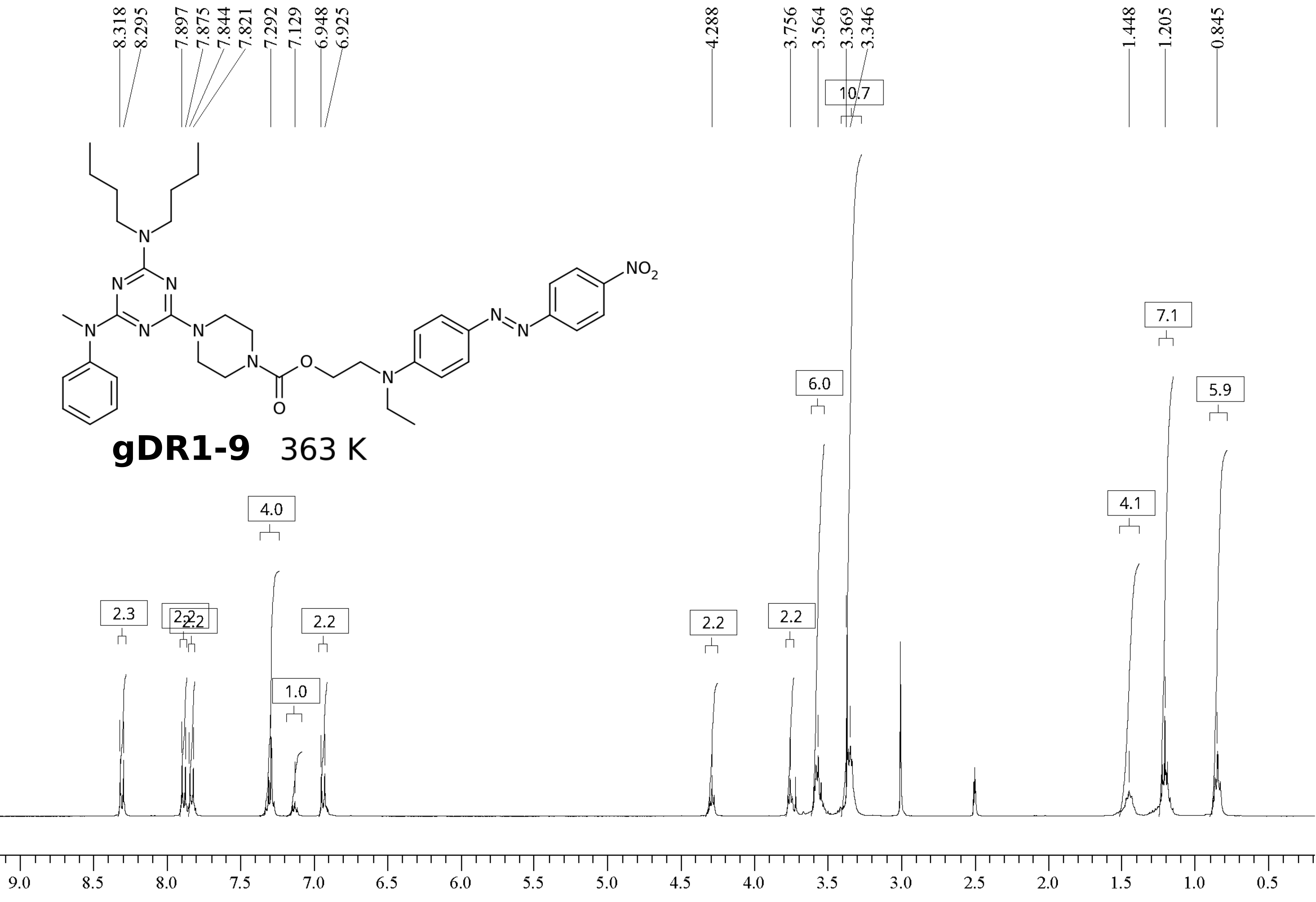

8.318
8.295
7.897
7.875
7.844
7.821
7.292
7.129
6.948
6.925
4.288
3.756
3.564
3.369
3.346
1.448
1.205
0.845
10.7
7.1
6.0
5.9
4.0
4.1
2.3
2.2
2.2
2.2
1.0
2.2
2.2
NO2
N
O
gDR1-9
363 K
9.0
8.5
8.0
7.5
7.0
6.5
6.0
5.5
5.0
4.5
4.0
3.5
3.0
2.5
2.0
1.5
1.0
0.5

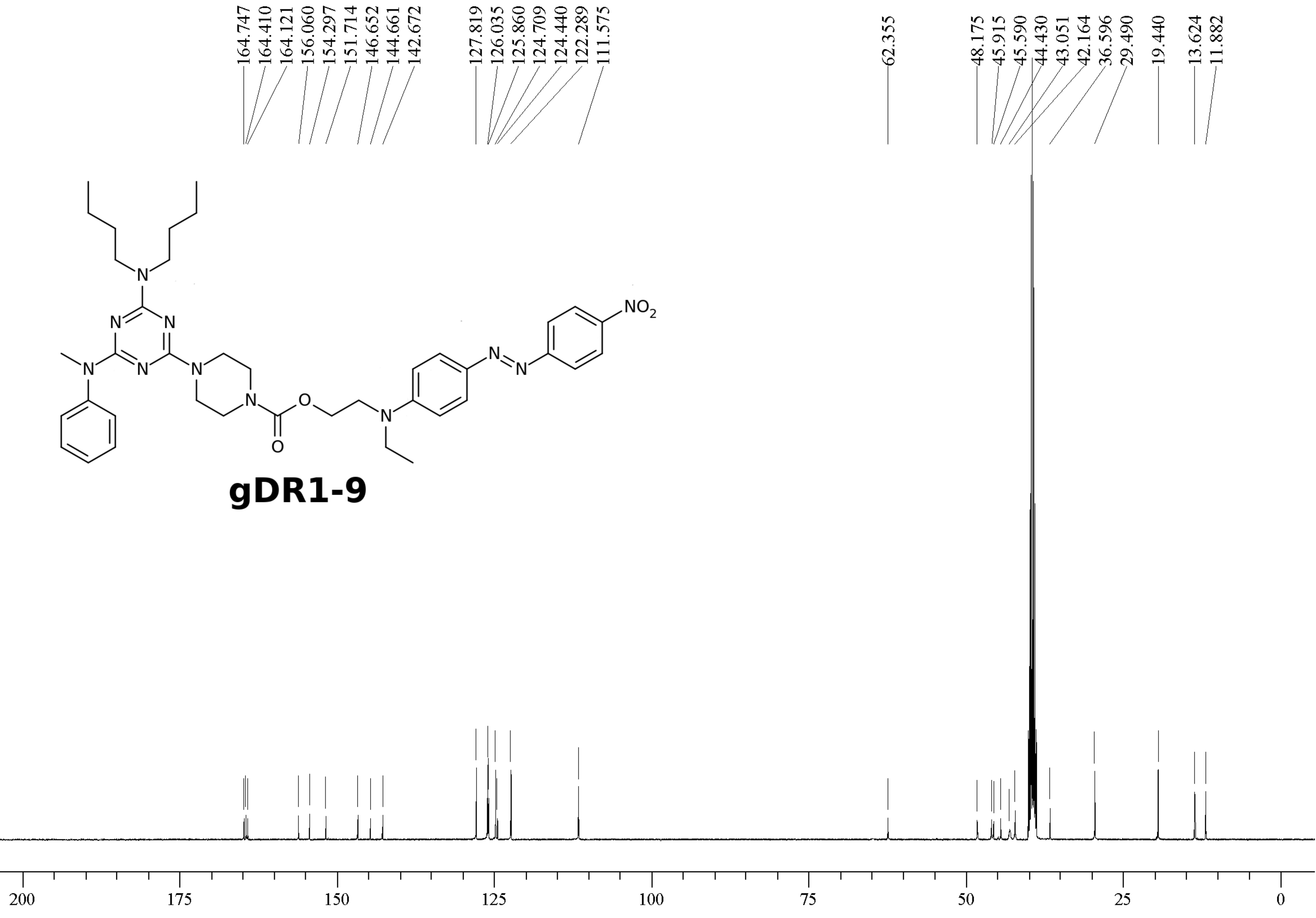

164.747
164.410
164.121
156.060
154.297
151.714
146.652
144.661
142.672
127.819
126.035
125.860
124.709
124.440
122.289
111.575
62.355
48.175
45.915
45.590
44.430
43.051
42.164
36.596
29.490
19.440
13.624
11.882
NO_2
200
175
150
125
100
75
50
25
0

gDR1-9

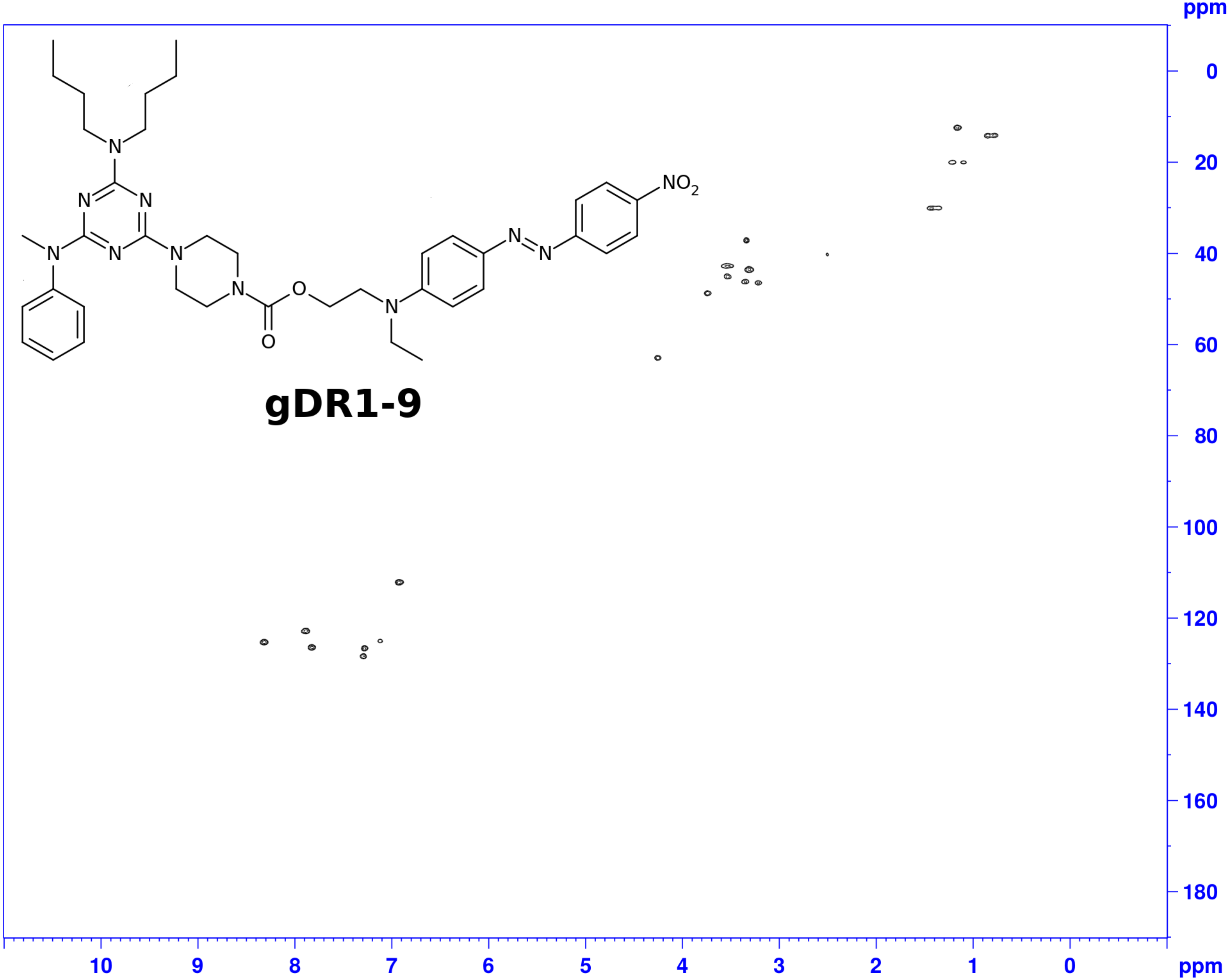
gDR1-9
ppm
0
20
40
60
80
100
120
140
160
180
ppm
10
9
8
7
6
5
4
3
2
1
0

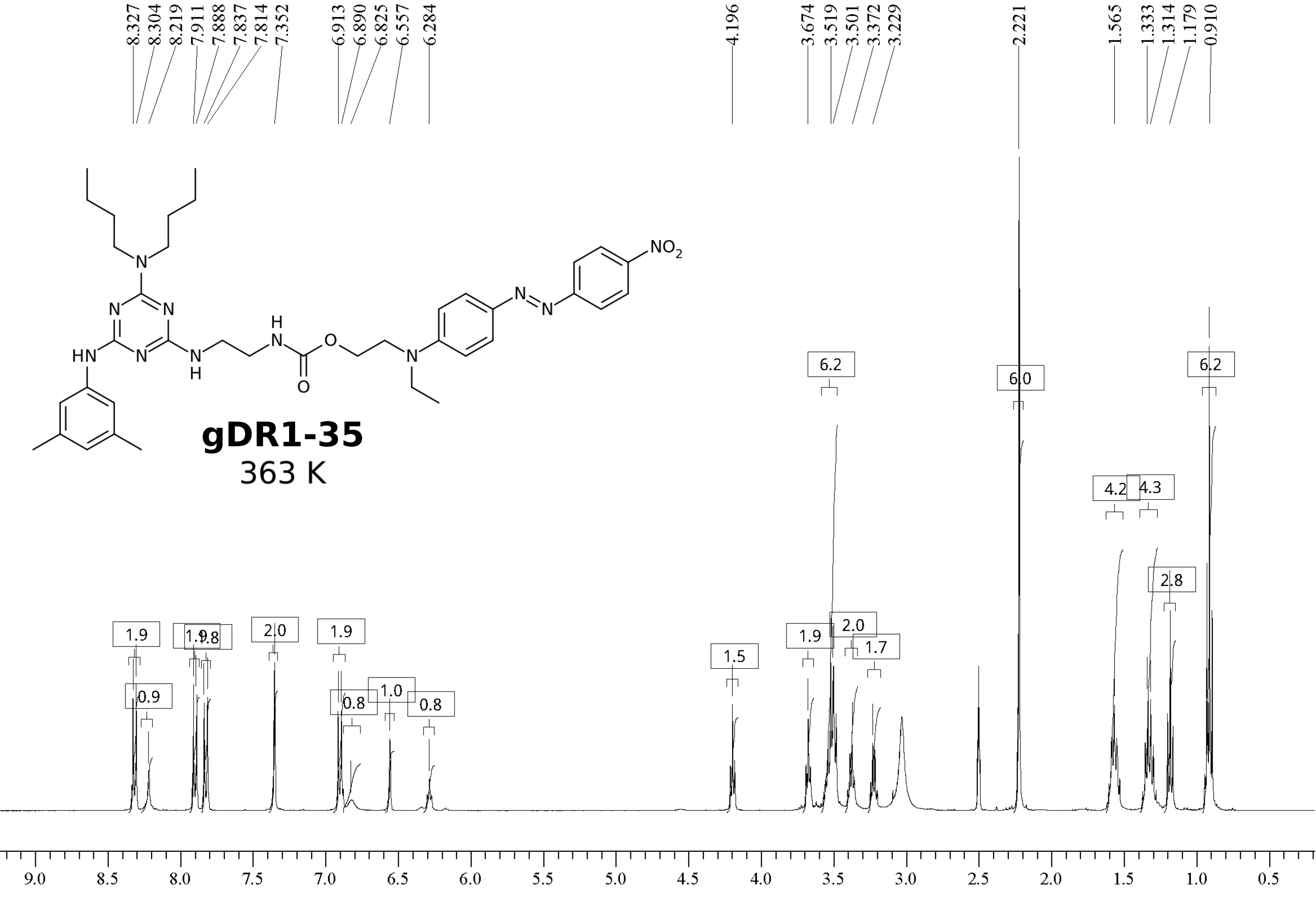
8.327
8.304
8.219
7.911
7.888
7.837
7.814
7.352
6.913
6.890
6.825
6.557
6.284
4.196
3.674
3.519
3.501
3.372
3.229
2.221
1.565
1.333
1.314
1.179
0.910
NO2
gDR1-35
363 K
1.9
0.9
1.9
1.8
2.0
1.9
0.8
1.0
0.8
1.5
1.9
6.2
2.0
1.7
6.0
4.2
4.3
2.8
6.2
9.0
8.5
8.0
7.5
7.0
6.5
6.0
5.5
5.0
4.5
4.0
3.5
3.0
2.5
2.0
1.5
1.0
0.5

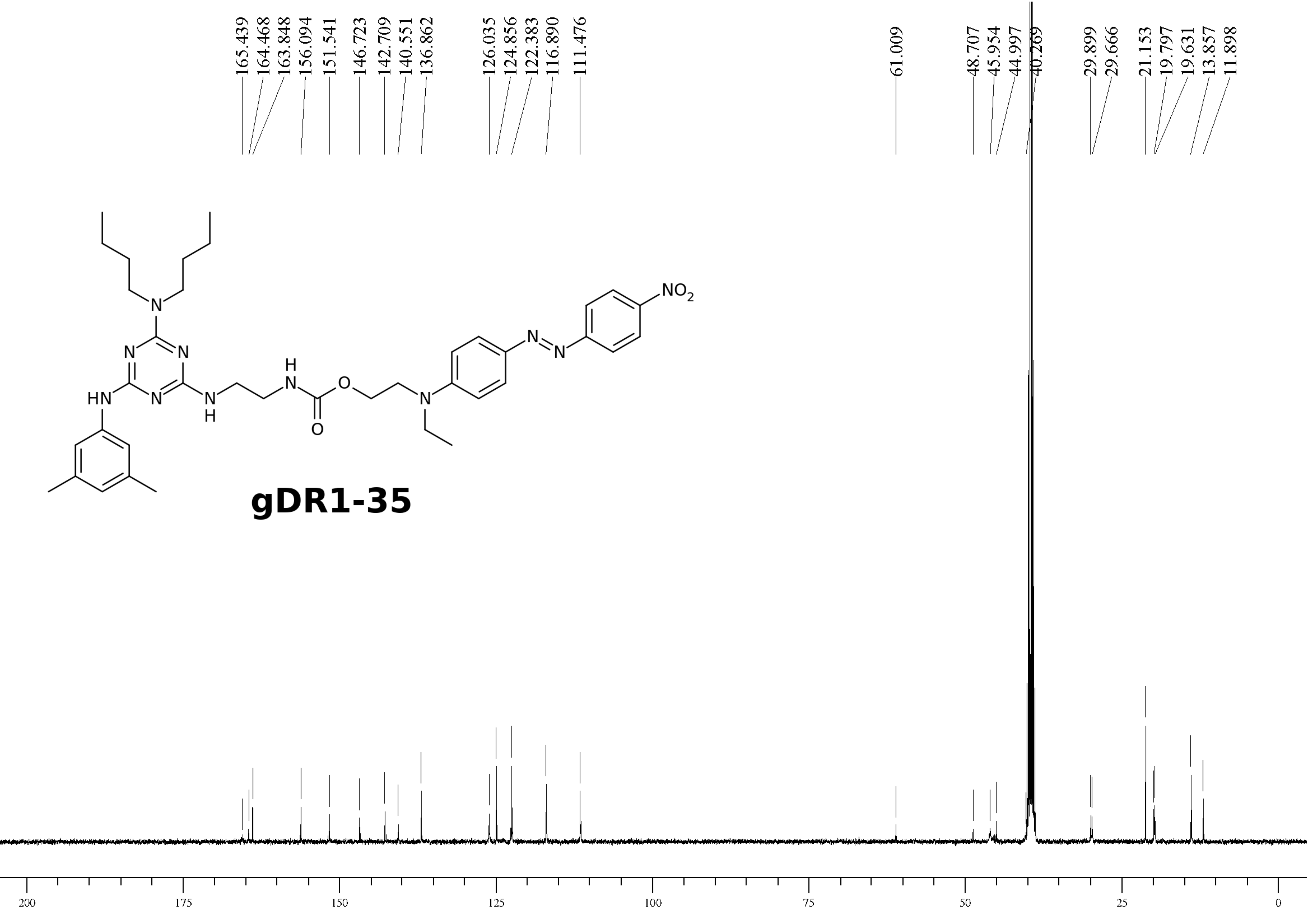
165.439
164.468
163.848
156.094
151.541
146.723
142.709
140.551
136.862
126.035
124.856
122.383
116.890
111.476
61.009
48.707
45.954
44.997
40.269
29.899
29.666
21.153
19.797
19.631
13.857
11.898
HN
N
N
N
N
H
N
H
O
O
N
N
N
NO_2
200
175
150
125
100
75
50
25
0

gDR1-35

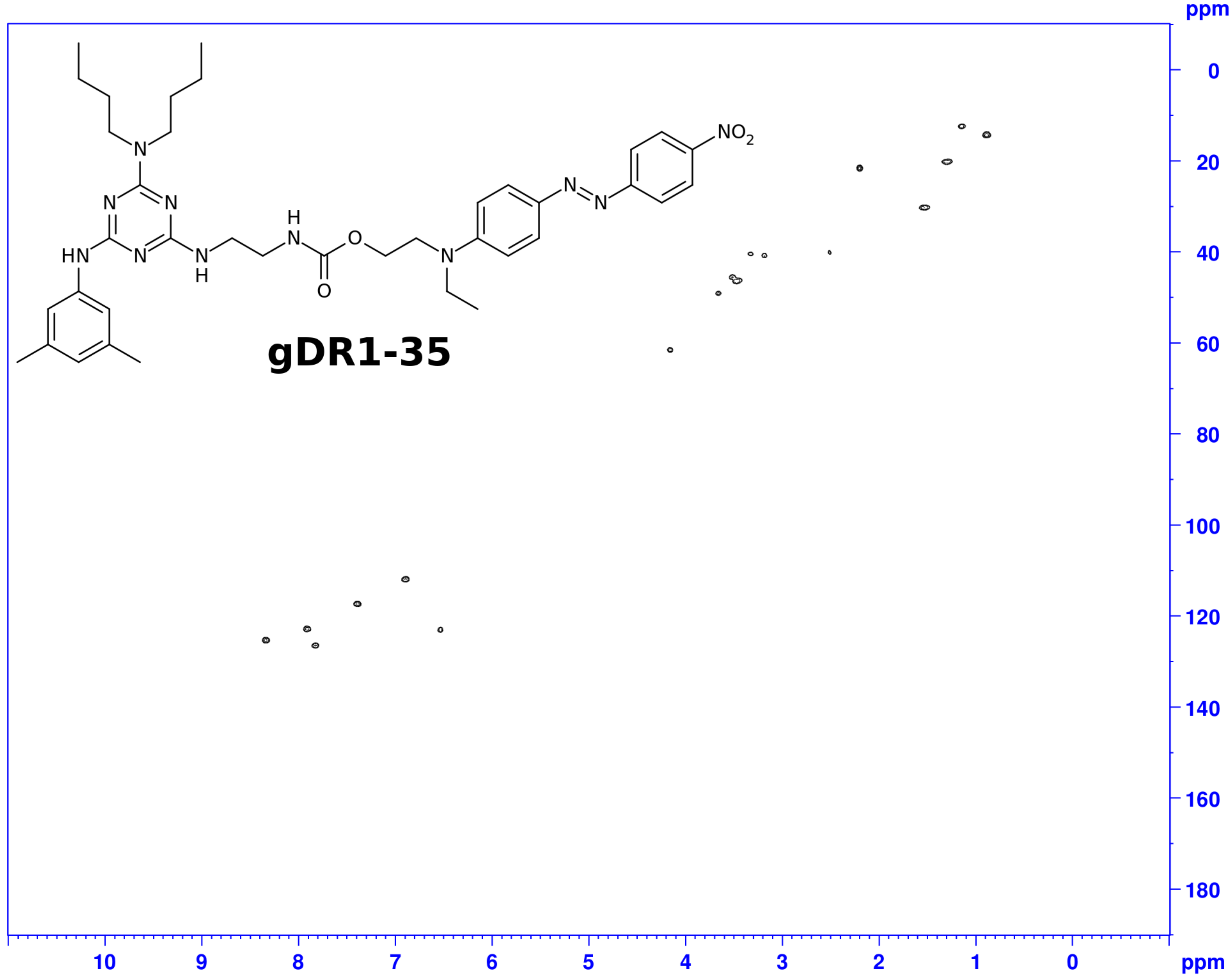
gDR1-35
ppm
0
20
40
60
80
100
120
140
160
180
10
9
8
7
6
5
4
3
2
1
0
ppm

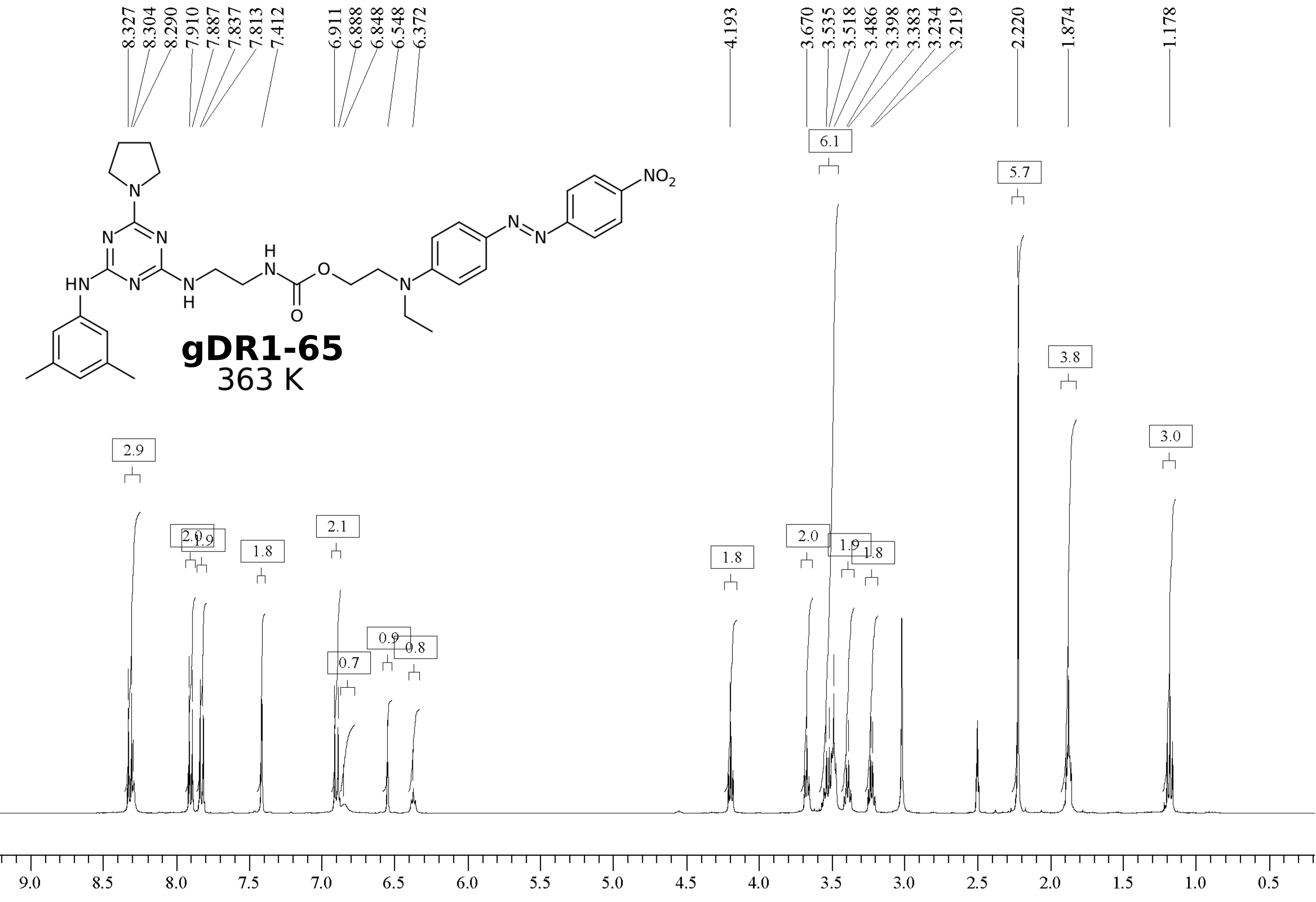

8.327
8.304
8.290
7.910
7.887
7.837
7.813
7.412
6.911
6.888
6.848
6.548
6.372
4.193
3.670
3.535
3.518
3.486
3.398
3.383
3.234
3.219
2.220
1.874
1.178
gDR1-65
363 K
2.9
2.0
1.9
1.8
2.1
0.7
0.9
0.8
1.8
2.0
6.1
1.9
1.8
5.7
3.8
3.0
9.0
8.5
8.0
7.5
7.0
6.5
6.0
5.5
5.0
4.5
4.0
3.5
3.0
2.5
2.0
1.5
1.0
0.5

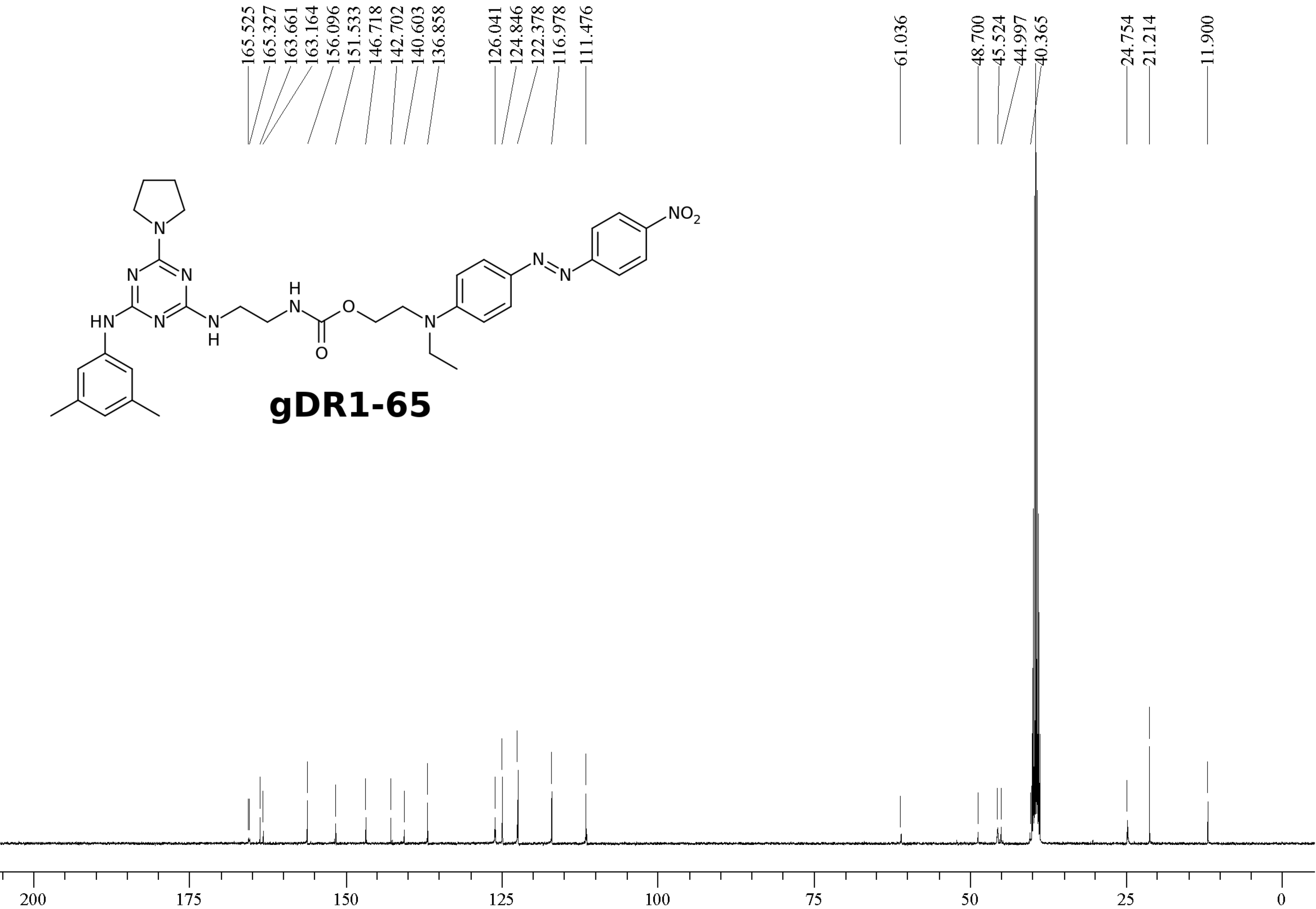
165.525
165.327
163.661
163.164
156.096
151.533
146.718
142.702
140.603
136.858
126.041
124.846
122.378
116.978
111.476
61.036
48.700
45.524
44.997
40.365
24.754
21.214
11.900
gDR1-65
200
175
150
125
100
75
50
25
0

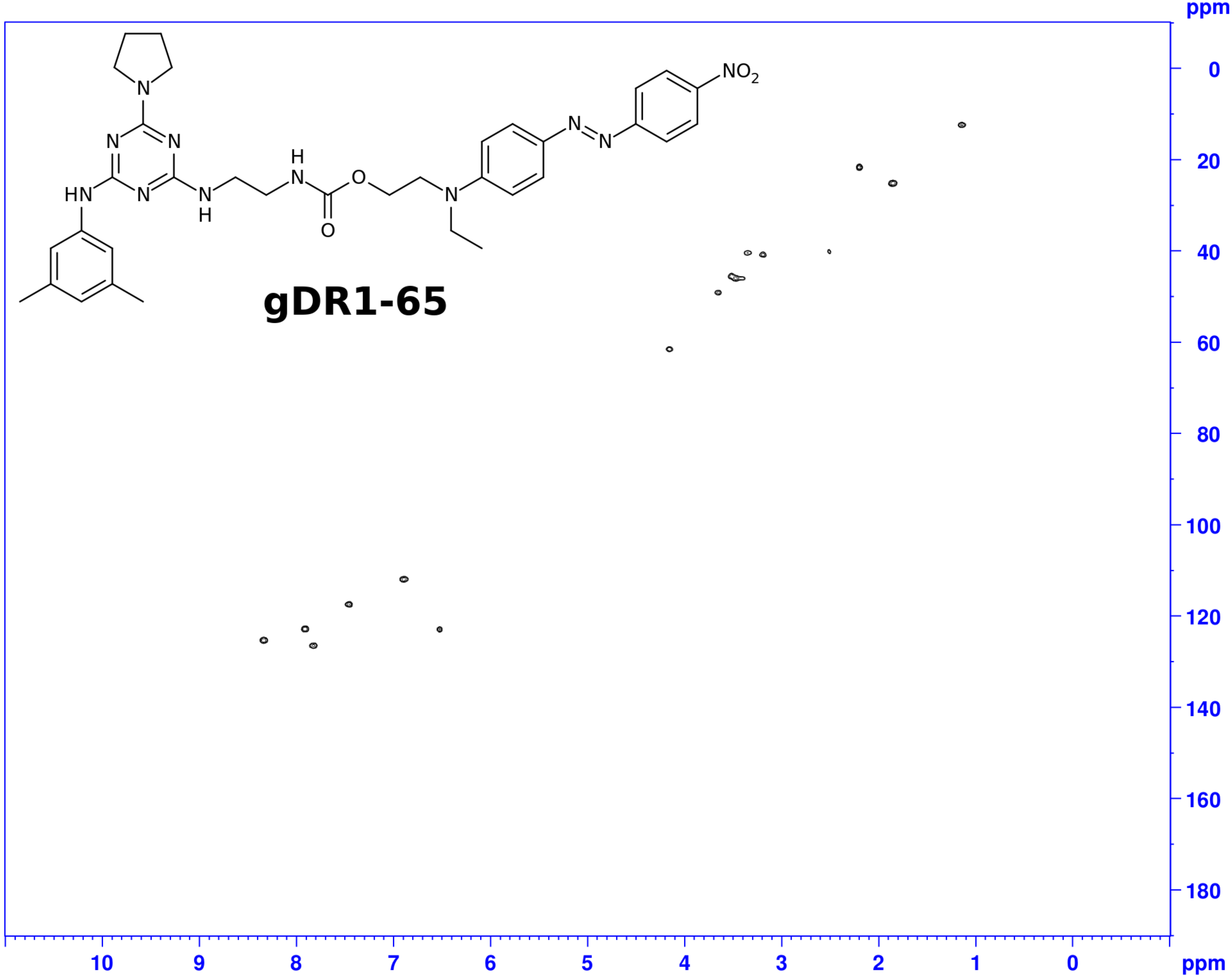

gDR1-65